



# Distinguishing early-stage nasopharyngeal carcinoma from benign hyperplasia using intravoxel incoherent motion diffusion-weighted MRI

Qi-Yong Ai<sup>1</sup> · Ann D. King<sup>1</sup> · Janet S. M. Chan<sup>1</sup> · Weitian Chen<sup>1</sup> · K. C. Allen Chan<sup>2</sup> · John K. S. Woo<sup>3</sup> · Benny C. Y. Zee<sup>4</sup> · Anthony T. C. Chan<sup>5</sup> · Darren M. C. Poon<sup>5</sup> · Brigitte B. Y. Ma<sup>5</sup> · Edwin P. Hui<sup>5</sup> · Anil T. Ahuja<sup>1</sup> · Alexander C. Vlantis<sup>3</sup> · Jing Yuan<sup>6</sup>

Received: 20 November 2018 / Revised: 14 February 2019 / Accepted: 6 March 2019 / Published online: 22 March 2019  
© European Society of Radiology 2019

## Abstract

**Objectives** MRI can detect early-stage nasopharyngeal carcinoma (NPC), but the detection is more challenging in early-stage NPCs because they must be distinguished from benign hyperplasia in the nasopharynx. This study aimed to determine whether intravoxel incoherent motion diffusion-weighted imaging (IVIM DWI) MRI could distinguish between these two entities.

**Methods** Thirty-four subjects with early-stage NPC and 30 subjects with benign hyperplasia prospectively underwent IVIM DWI. The mean pure diffusion coefficient ( $D$ ), pseudo-diffusion coefficient ( $D^*$ ), perfusion fraction ( $f$ ) and apparent diffusion coefficient (ADC) values were calculated for all subjects and compared between the 2 groups using Student's  $t$  test. Receiver operating characteristics with the area under the curve (AUC) was used to identify the optimal threshold for all significant parameters, and the corresponding diagnostic performance was calculated. A  $p$  value of  $<0.05$  was considered statistically significant.

**Results** Compared with benign hyperplasia, early-stage NPC exhibited a significantly lower  $D$  mean ( $0.64 \pm 0.06$  vs  $0.87 \pm 0.11 \times 10^{-3} \text{ mm}^2/\text{s}$ ),  $\text{ADC}_{0-1000}$  mean ( $0.77 \pm 0.08$  vs  $1.00 \pm 0.13 \times 10^{-3} \text{ mm}^2/\text{s}$ ),  $\text{ADC}_{300-1000}$  ( $0.63 \pm 0.05$  vs  $0.86 \pm 0.10 \times 10^{-3} \text{ mm}^2/\text{s}$ ) and a higher  $D^*$  mean ( $32.66 \pm 4.79$  vs  $21.96 \pm 5.21 \times 10^{-3} \text{ mm}^2/\text{s}$ ) (all  $p < 0.001$ ). No significant difference in the  $f$  mean was observed between the two groups ( $p = 0.216$ ). The  $D$  and  $\text{ADC}_{300-1000}$  mean had the highest AUC of 0.985 and 0.988, respectively, and the  $D$  mean of  $<0.75 \times 10^{-3} \text{ mm}^2/\text{s}$  yielded the highest sensitivity, specificity and accuracy (100%, 93.3% and 96.9%, respectively) in distinguishing early-stage NPC from benign hyperplasia.

**Conclusion** DWI has potential to distinguish early-stage NPC from benign hyperplasia and  $D$  and  $\text{ADC}_{300-1000}$  mean were the most promising parameters.

## Key Points

- Diffusion-weighted imaging has potential to distinguish early-stage nasopharyngeal carcinoma from benign hyperplasia in the nasopharynx.
- The pure diffusion coefficient, pseudo-diffusion coefficient from intravoxel incoherent motion model and apparent diffusion coefficient from conventional diffusion-weighted imaging were significant parameters for distinguishing these two entities in the nasopharynx.
- The pure diffusion coefficient, followed by apparent diffusion coefficient, may be the most promising parameters to be used in screening studies to help detect early-stage nasopharyngeal carcinoma.

**Keywords** Diffusion magnetic resonance imaging · Nasopharyngeal carcinoma · Hyperplasia

✉ Ann D. King  
king2015@cuhk.edu.hk

## Abbreviations

ADC	Apparent diffusion coefficient
AUC	Area under the curve
CI	Confidence interval
<i>D</i>	Pure diffusion coefficient
<i>D</i> *	Pseudo-diffusion coefficient
DWI	Diffusion-weighted imaging
EBV	Epstein–Barr virus
<i>f</i>	Perfusion volume fraction
ICC	Intra-class correlation coefficient
IVIM	Intravoxel incoherent motion
NPC	Nasopharyngeal carcinoma

## Introduction

Benign hyperplasia causes generalised thickening of the mucosa/submucosa along the nasopharyngeal walls and enlargement of the adenoid and is a common incidental finding on MRI of the adult head and neck, as well as on brain imaging [1]. Benign hyperplasia may need to be distinguished from early-stage nasopharyngeal carcinoma (NPC) confined to the nasopharynx. This is especially relevant in NPC endemic regions because the current trend of using plasma Epstein–Barr virus (EBV) DNA to screen asymptomatic subjects for NPC has led to an increase in the number of tumours detected at an early stage [2]. In most cases, these entities can be distinguished using anatomical images; lymphoid hyperplasia causes diffuse wall thickening symmetrically involving both sides of the nasopharynx, and when there is hyperplasia of the adenoid, the adenoidal stripes tend to be preserved, whereas early-stage NPC tends to cause a focal mass and loss or distortion of the adenoidal stripes [1, 3, 4]. However, in a small number of patients, lymphoid hyperplasia may cause asymmetrical thickening and the adenoidal stripes may not be identified, especially if the scan is not a dedicated scan of the nasopharynx. Furthermore, we have shown recently that 12% of stage T1 NPCs cause diffuse symmetrical thickening of the nasopharyngeal walls similar to that in benign hyperplasia [4].

The ability of MRI to accurately distinguish benign hyperplasia from NPC is also becoming more important because MRI is used more frequently to detect the 10% of NPCs that are occult on the endoscopic examination [3]. The detection of NPC by MRI is even more challenging in the screening setting, wherein plasma markers such as EBV DNA are used to identify early-stage NPCs in asymptomatic subjects [2].

Diffusion-weighted imaging (DWI) can distinguish benign from malignant head and neck tumours [5] and intravoxel incoherent motion (IVIM) DWI may be superior to conventional DWI for tissue characterisation, as the former can distinguish the process of pure diffusion from microcirculation in the capillary network. Indeed, an early study reported that IVIM DWI

could distinguish NPC from benign adenoids in the nasopharynx [6]. If IVIM DWI is useful in the screening setting, it would not only improve the diagnostic performance of the current MRI protocol but potentially could replace the T1 contrast-enhanced scan which could expand the use of MRI.

Therefore, this preliminary study hypothesised that DWI has the potential to distinguish benign hyperplasia from early-stage NPC. This study was designed to examine whether IVIM-derived parameters, together with apparent diffusion coefficient (ADC) obtained from conventional DWI, are able to distinguish benign hyperplasia from early-stage NPC. The second part of the study compared diagnostic performance of these DW parameters to examine whether IVIM DWI had advantages over the conventional DWI in distinguishing between these two entities in the nasopharynx.

## Methods

### Patients

This prospective study was performed under approval from the local institutional review board. The patients were ethnically Chinese who were recruited between March 2015 and July 2018, and written informed consent was obtained from all patients.

### Patients with early-stage NPC

Consecutive symptomatic and asymptomatic patients who met the following criteria were included: (1) newly diagnosed, biopsy-proven undifferentiated NPC; (2) primary tumour confined to the nasopharynx (stage T1) on MRI without superficial spread to the nasal cavity or oropharynx or deep spread within the nasopharynx; and (3) a primary tumour size > 5 mm.

### Patients with benign hyperplasia

Consecutive asymptomatic patients who were undergoing follow-up investigations for benign hyperplasia were recruited from a previous NPC detection study with persistently raised plasma EBV DNA [2] who met the following criteria: (1) did not have NPC after the initial endoscopic examination and contrast-enhanced MRI and showed no change suggestive of NPC on the follow-up endoscopic examination and non-contrast-enhanced MRI two years later; (2) follow-up MRI examination showed benign hyperplasia > 5 mm in thickness.

### MRI acquisition

MRI was performed using a Philips Achieva TX 3.0-T scanner (Philips Healthcare) with a body coil for radiofrequency transmission and a 16-channel Philips neurovascular phased-array

coil for reception. IVIM DWI was acquired using a fat-suppressed, single-shot, spin-echo, echo-planar imaging sequence (number of slices: 9, repetition time/echo time, 2000/50 ms; field of view, 230 mm × 230 mm; section thickness, 4 mm; echo train length, 55; sensitivity encoding factor, 2; number of signals acquired, 4) and 14 *b*-values (0, 20, 40, 50, 60, 80, 100, 200, 300, 400, 500, 600, 800 and 1000 s/mm<sup>2</sup>). The total IVIM DWI scan time was 2 min, 30 s.

Anatomical MRI in all patients included a fat-suppressed T2-weighted turbo-spin-echo sequence and a T1-weighted turbo-spin-echo sequence. The patients with early-stage NPC were also scanned using a T1-weighted turbo-spin-echo sequence following a bolus injection of 0.1 mmol of gadoteric acid (Dotarem; Guerbet) per kilogramme of body weight.

### Imaging analysis

Olea Sphere (version 3.0; Olea Medical SA) was used for all the post-processing steps by implementing a Bayesian probability-based algorithm using all 14 *b*-values to fit a bi-exponential diffusion model to calculate the pure diffusion coefficient (*D*); the pseudo-diffusion coefficient (*D*\*), which reflects blood microcirculation in the capillary networks; and the perfusion volume fraction (*f*), which correlates with capillary geometry and blood velocity [7], and using six *b*-values (0, 200, 400, 600, 800, 1000 s/mm<sup>2</sup>) to fit a mono-exponential diffusion model to calculate the conventional ADC (ADC<sub>0–1000</sub>). In addition, *b*-values of 300, 400, 600, 800 and 1000 s/mm<sup>2</sup> were used to fit a mono-exponential diffusion model for the purpose of comparing conventional ADC<sub>300–1000</sub> with *D* in the IVIM model. On the ADC map, the region of interest was manually drawn around the whole primary tumour or benign hyperplasia with reference to the corresponding anatomical images by a radiologist with more than 20 years of experience with specialisation in the head and neck region and a researcher with 4 years of experience of treating NP disease. The region of interest on the ADC map was then fitted automatically to the other diffusion maps. Necrotic and cystic regions were excluded from the analysis during the delineation phase. The total volume of the abnormalities in the nasopharynx was

obtained by manually outlining the cross-sectional area on each slice, summing the cross-sectional areas, and multiplying by the slice thickness of 4 mm.

### Statistical analysis

Distributions of DW parameters in the early-stage NPC and benign hyperplasia groups were examined using Kolmogorov–Smirnov test. Differences in the DW parameters between the two groups were compared using Student's *t* test (data normally distributed) or Mann–Whitney *U* test (data not normally distributed). A receiver-operating characteristic curve analysis and subsequent area under the curve (AUC) calculation were used to identify the optimal thresholds for the significant DW parameters by maximising the sensitivity plus specificity, and the diagnostic performance of these thresholds was calculated and the significance of these thresholds was re-evaluated with the chi-square test. The AUCs of significant DW parameters were compared using the Delong test. The above analyses used the average values of the parameters obtained from the 2 observers. Intra-class correlation coefficients (ICCs) with 95% confidence intervals (95% CIs) were calculated to assess the inter-observer agreement regarding the IVIM-derived parameters and ADC<sub>0–1000</sub>. ICC was also calculated to assess the agreement between *D* from the IVIM model and ADC<sub>300–1000</sub>.

All of the statistical tests were 2-sided, and a *p* value < 0.05 was considered to indicate a statistically significant difference. Analyses were performed using the statistical analysis software SPSS (version 25.0; IBM) and MedCalc Statistical Software (version 14.8.1; MedCalc Software).

## Results

### Patients

Thirty-nine patients with early-stage NPC confined to the nasopharynx and 32 patients with benign hyperplasia were recruited. Of these, 7 were excluded because of degraded

**Table 1** Characteristics of the 64 included subjects

Clinical characteristics	Early-stage nasopharyngeal carcinoma ( <i>n</i> = 34)	Benign hyperplasia ( <i>n</i> = 30)
Age (years)	50.8 ± 12.3 (25–80)*	53.4 ± 6.9 (42–64)*
Gender		
Male	29	30
Female	5	0
Abnormality minimum diameter (mm)	10.7 ± 3.7 (5.2–20.7)*	7.7 ± 2.1 (5.1–12.7) *
Total volume (cm <sup>3</sup> )	5.87 ± 2.94 (2.46–13.10)	4.55 ± 1.14 (2.58–6.92)

\*Data are presented as means ± standard deviations (ranges)

**Table 2** Analysis of DW parameters calculated for study subjects

	All subjects ( $n = 64$ )	Early-stage NPC ( $n = 34$ )	Benign hyperplasia ( $n = 30$ )	$p$ value (early-stage NPC vs. benign hyperplasia)
$D$ mean ( $\times 10^{-3}$ mm <sup>2</sup> /s)	$0.75 \pm 0.14$ (0.55–1.12)	$0.64 \pm 0.06$ (0.55–0.74)	$0.87 \pm 0.11$ (0.68–1.12)	$< 0.001$
$D^*$ mean ( $\times 10^{-3}$ mm <sup>2</sup> /s)	$27.57 \pm 7.21$ (10.17–39.66)	$32.66 \pm 4.79$ (21.22–39.66)	$21.96 \pm 5.21$ (10.17–35.80)	$< 0.001$
$f$ mean	$0.11 \pm 0.04$ (0.05–0.26)	$0.10 \pm 0.03$ (0.05–0.19)	$0.11 \pm 0.04$ (0.07–0.26)	0.216
ADC <sub>0–1000</sub> mean ( $\times 10^{-3}$ mm <sup>2</sup> /s)	$0.88 \pm 0.16$ (0.64–1.29)	$0.77 \pm 0.08$ (0.64–0.98)	$1.00 \pm 0.13$ (0.80–1.29)	$< 0.001$
ADC <sub>300–1000</sub> mean ( $\times 10^{-3}$ mm <sup>2</sup> /s)	$0.74 \pm 0.14$ (0.53–1.07)	$0.63 \pm 0.05$ (0.53–0.78)	$0.86 \pm 0.10$ (0.70–1.07)	$< 0.001$

A  $p$  value  $< 0.05$  (italicised) indicates statistical significance. Data are presented as means  $\pm$  standard deviations (ranges)

DW parameter = diffusion-weighted parameter, NPC = nasopharyngeal carcinoma, ADC = apparent diffusion coefficient

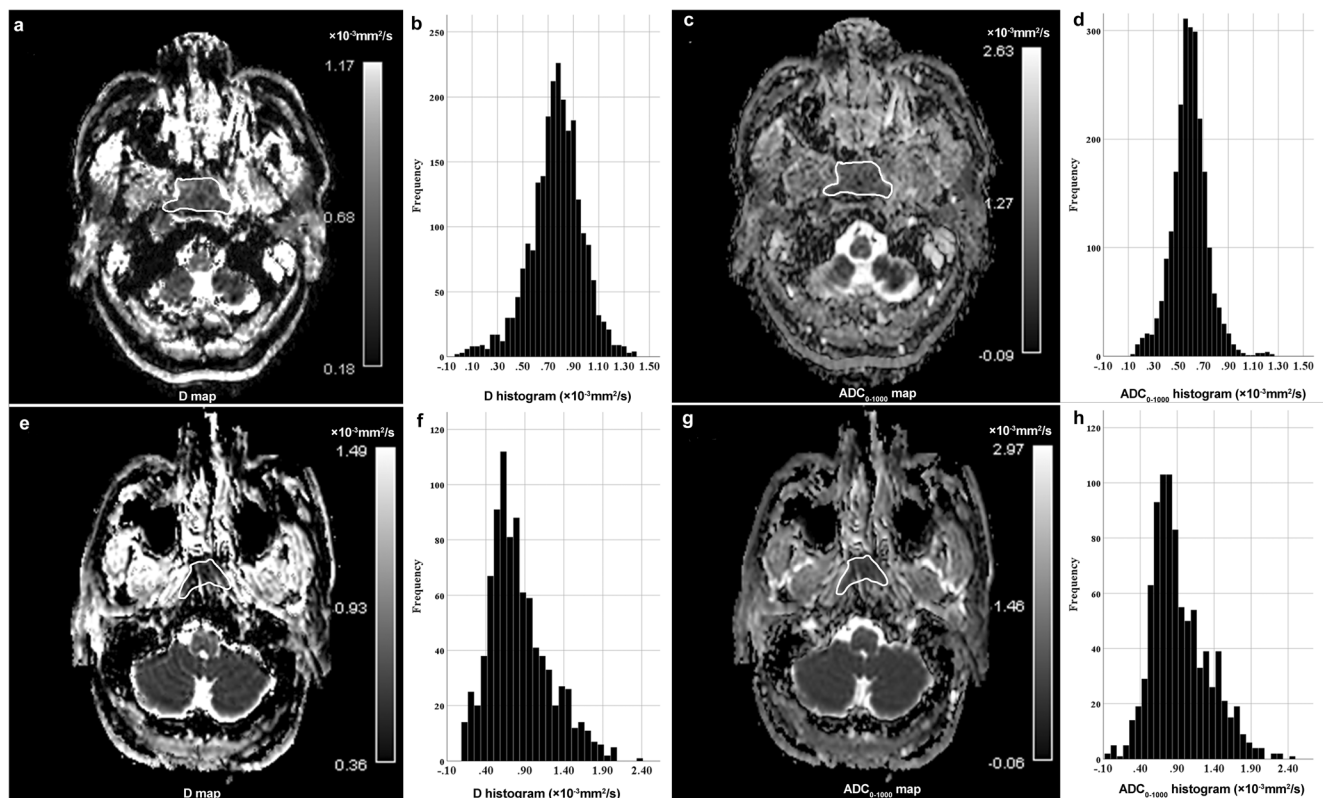
images (NPC = 5 and benign hyperplasia = 2). The characteristics of the remaining 34 patients with NPC and 30 patients with benign hyperplasia are shown in Table 1.

### DW parameters

The DW parameters of subjects with early-stage NPC and benign hyperplasia are shown in Table 2. DW parameters in each group was normally distributed ( $p = 0.072$ – $0.200$ ), and compared with the subjects with benign hyperplasia; those

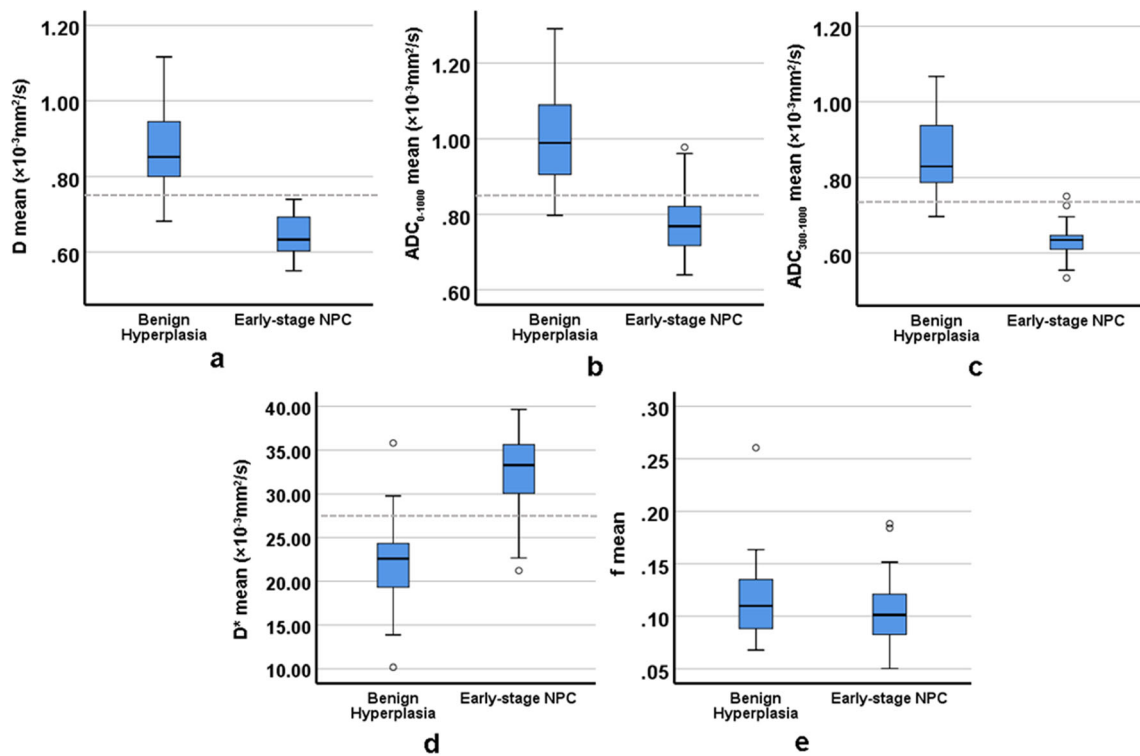
with early-stage NPC had significantly lower  $D$  mean, ADC<sub>0–1000</sub> mean (Fig. 1) and ADC<sub>300–1000</sub> mean values (Fig. 2a–c, Table 2) and a higher  $D^*$  mean value (Fig. 2d, Table 2). However, no significant inter-group difference was observed in the  $f$  mean values (Fig. 2e, Table 2).

Table 3 and Fig. 3 present the diagnostic performance of the optimal thresholds for the above-listed significant DW parameters, as well as the AUCs of these parameters for distinguishing early-stage NPC from benign hyperplasia. Notably, the  $D$  mean was best able to distinguish these two entities in the nasopharynx,



**Fig. 1** Pure diffusion ( $D$ ) and apparent diffusion coefficient<sub>0–1000</sub> (ADC<sub>0–1000</sub>) maps and histograms of a representative subject with early-stage nasopharyngeal carcinoma (NPC) (a–d) and a representative subject with benign hyperplasia in the nasopharynx (e–h). The respective

$D$  mean and ADC<sub>0–1000</sub> mean values were  $0.59 \times 10^{-3}$  mm<sup>2</sup>/s (b) and  $0.82 \times 10^{-3}$  mm<sup>2</sup>/s (d) for the subject with early-stage NPC and  $0.76 \times 10^{-3}$  mm<sup>2</sup>/s (f) and  $0.93 \times 10^{-3}$  mm<sup>2</sup>/s (h) for the subject with benign hyperplasia



**Fig. 2** Side-by-side box plots of the mean true diffusion coefficient (*D*), apparent diffusion coefficient<sub>0–1000</sub> (ADC<sub>0–1000</sub>), ADC<sub>300–1000</sub>, pseudo-diffusion (perfusion) coefficient (*D*<sup>\*</sup>) and perfusion volume fraction (*f*) values in subjects with early-stage nasopharyngeal carcinoma (NPC) and benign hyperplasia. Patients with early-stage NPC had a significant lower *D* mean (a), ADC<sub>0–1000</sub> mean (b) and ADC<sub>300–1000</sub> (c), and a significantly

higher *D*<sup>\*</sup> mean (d), compared to patients with benign hyperplasia. The difference in the *f* mean (e) between the two groups was not significant. The optimal thresholds (grey dotted lines) of *D* mean, ADC<sub>0–1000</sub> mean, ADC<sub>300–1000</sub> and *D*<sup>\*</sup> mean for distinguishing early-stage NPC from benign hyperplasia were  $0.75 \times 10^{-3} \text{ mm}^2/\text{s}$ ,  $0.74 \times 10^{-3} \text{ mm}^2/\text{s}$ ,  $0.86 \times 10^{-3} \text{ mm}^2/\text{s}$  and  $27.4 \times 10^{-3} \text{ mm}^2/\text{s}$ , respectively

although when compared to ADC<sub>0–1000</sub> mean and *D*<sup>\*</sup> mean, there were no significant differences between the AUCs. Analysis of the inter-observer agreement yielded the highest ICC values for the *D* mean and ADC<sub>0–1000</sub> mean (0.963 (95%

CI, 0.940–0.978)), followed by the *D*<sup>\*</sup> mean (0.953 (95% CI, 0.922–0.971)), and *f* mean (0.920 (95% CI, 0.868–0.951)) (all  $p < 0.001$ ). The ADC<sub>300–1000</sub> mean had a similar threshold and AUC (Table 3 and Fig. 3) ( $p = 0.823$ ) to the *D* mean for

**Table 3** Diagnostic performance of DW parameters in distinguishing early-stage NPC from benign hyperplasia

	<i>D</i> mean	<i>D</i> <sup>*</sup> mean	ADC <sub>300–1000</sub> mean	ADC <sub>0–1000</sub> mean
AUC (95% CI)	0.985 (0.962–1.000)	0.926 (0.858–0.995)	0.988 (0.969–1.000)	0.948 (0.900–0.996)
<i>p</i> value	<0.001	<0.001	<0.001	<0.001
Threshold ( $\times 10^{-3} \text{ mm}^2/\text{s}$ )	<0.75	>27.40	<0.74	<0.86
TP	34	29	33	29
FP	2	3	2	3
TN	28	27	28	27
FN	0	5	1	5
Sensitivity	100.0%	85.3%	97.0%	85.3%
Specificity	93.3%	90.0%	93.3%	90.0%
PPV	94.4%	90.9%	94.3%	90.9%
NPV	100.0%	81.8%	96.6%	81.8%
Accuracy	96.9%	86.4%	95.3%	86.4%

A *p* value of <0.05 indicates statistical significance

*DW parameter* = diffusion-weighted parameter, *NPC* = nasopharyngeal carcinoma, *AUC* = area under the curve, *ADC* = apparent diffusion coefficient, *TP* = true positive, *FP* = false positive, *TN* = true negative, *FN* = false negative, *PPV* = positive predictive value. *NPV* = negative predictive value

distinguishing early-stage NPC from benign hyperplasia with a high ICC of 0.968 (95% CI, 0.948–0.981).

## Discussion

MRI has been established as the imaging modality of choice for the staging of biopsy-proven NPC [8, 9]. However, the role of this imaging modality is expanding to include the detection of endoscopically occult tumours [3, 10]. As a result of the more widespread use of plasma markers to screen for early-stage NPC, there is increasing pressure on MRI to distinguish benign hyperplasia from early-stage cancers which do not have other features such as deep spread or nodal metastases to suggest malignancy on MRI. Therefore, an MRI sequence that could improve the diagnostic performance of anatomical imaging and even replace contrast-enhanced images would be advantageous in the screening setting.

In this study, the mean values of the IVIM-derived parameters  $D$  and  $D^*$ , but not  $f$ , could successfully distinguish early-stage NPC from benign hyperplasia.  $D$  mean was significantly lower and  $D^*$  significantly higher in NPC than in benign hyperplasia suggesting NPC has hyper-cellularity, smaller extracellular space and more vascularity than benign hyperplasia. Of these two parameters, the  $D$  mean yielded the best diagnostic performance and reproducibility, but  $ADC_{0-1000}$  from a conventional DWI was also useful. Similar to  $D$ , subjects with early-stage NPC had a significantly lower  $ADC_{0-1000}$  than those with benign hyperplasia, suggesting that pure diffusion, compared with microcirculation, more strongly influences the  $ADC_{0-1000}$  value. Although the accuracy of  $ADC_{0-1000}$  mean was slightly lower than that of  $D$ , conventional DWI is still an acceptable alternative to IVIM DWI for patients, especially for those patients unable to tolerate the longer time scan. Scan time could be further reduced by limiting the conventional DWI to only those  $b$ -values between 300 and 1000  $s/mm^2$  to acquire the  $ADC_{300-1000}$  which we found provided similar results to the  $D$  mean from the IVIM model. Our DWI results suggest that biopsies targeted to sites with a low  $D$  mean or low  $ADC_{300-1000}$  mean should have a high sensitivity for NPC, although a small number will be false positive because of an overlap in the mean values with benign hyperplasia. In addition, a turbo-spin-echo sequence, rather than an echo-planar sequence, can be used during conventional DW image acquisition. This is advantageous because the turbo-spin-echo sequence reduces susceptibility artefacts in the nasopharynx [11, 12].

DWI aids for the MRI-based characterisation of tissues in the head and neck. Most studies have reported lower ADC values in malignant tumours relative to benign processes, which reflects the more restricted diffusion in the former lesions [5]. More recently, IVIM studies in the head and neck have reported lower  $D$  values in malignant tumours relative to

benign pathologies [6, 13–19], including comparisons of NPC with benign hyperplasia [6], which are consistent with our findings. The previously reported values for  $D$  in NPC [6, 18–24] and benign hyperplasia [6, 25] were also similar to those in our study. This similarity is encouraging given that our prospective study of consecutive patients in a screening setting included those with small volumes of NPC and benign hyperplasia. The other two IVIM parameters,  $D^*$  and  $f$ , are likely less robust, which is supported by the greater range of values reported in studies of the head and neck [26], including NPC [6, 18–24].

This study had several limitations. Firstly, we were unable to assess whether there are differences in IVIM parameters between the two patterns of contrast enhancement in benign hyperplasia, because at the time of this IVIM study we only obtained plain scans in our patients who were undergoing follow-up MRI. Secondly, although the  $D$  mean yielded a superior diagnostic performance relative to the  $ADC_{0-1000}$  mean and  $D^*$  mean, these differences did not reach statistical significance, likely due to the small sample size. Thirdly, the optimal thresholds obtained in this preliminary study will require validation in an independent data set before implementation in clinical practice.

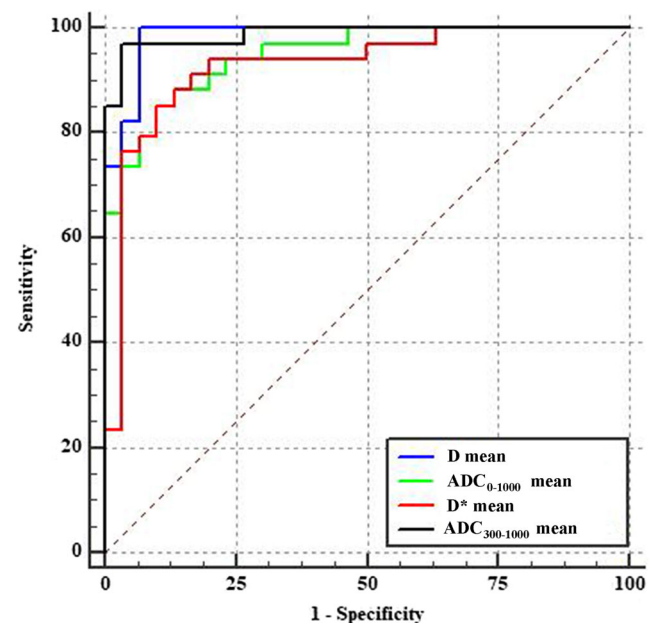


**Fig. 3** Analysis of areas under the curves (AUCs) of the mean values of the true diffusion coefficient ( $D$ ), pseudo-diffusion coefficient ( $D^*$ ), apparent diffusion coefficient<sub>0-1000</sub> ( $ADC_{0-1000}$ ) and  $ADC_{300-1000}$  to determine the ability to distinguish early-stage nasopharyngeal carcinoma from benign hyperplasia. The  $D$  mean and  $ADC_{300-1000}$  had the highest AUCs of 0.985 and 0.988, respectively (blue curve and black curve, respectively), followed by the  $ADC_{0-1000}$  mean (0.948; green curve) and  $D^*$  mean (0.926; red curve). This suggests that the  $D$  mean and  $ADC_{300-1000}$  were best able to distinguish early-stage nasopharyngeal carcinoma from benign hyperplasia

## Conclusion

In conclusion, the mean IVIM values of  $D$  and  $D^*$  but not  $f$ , together with the mean  $ADC_{0-1000}$  and  $ADC_{300-1000}$  values obtained from conventional DWI, were identified as potential DW parameters that could distinguish early-stage NPC from benign hyperplasia in the nasopharynx. NPC was associated with a lower  $D$ ,  $ADC_{0-1000}$ ,  $ADC_{300-1000}$  and a higher  $D^*$  compared with benign hyperplasia, with the  $D$  and  $ADC_{300-1000}$  being the most promising parameters for use in the screening setting.

**Funding** This study has received funding by the Research Grant Council of Hong Kong. The work described in this paper was partially supported by grants from the Research Grants council of the Hong Kong Special Administrative Region, China (Project No. 14107216 and SEG\_CUHK02).

## Compliance with ethical standards

**Guarantor** The scientific guarantor of this publication is Ann D King.

**Conflict of interest** The authors of this manuscript declare no relationships with any companies, whose products or services may be related to the subject matter of the article.

**Statistics and biometry** One of the authors has significant statistical expertise.

**Informed consent** Written informed consent was obtained from all subjects (patients) in this study.

**Ethical approval** Institutional Review Board approval was obtained.

**Study subjects or cohorts overlap** Some study subjects or cohorts have been previously reported in New England Journal of Medicine entitled “Analysis of Plasma Epstein-Barr Virus DNA to Screen for Nasopharyngeal Cancer” (doi: <https://doi.org/10.1056/NEJMoa1701717>).

## Methodology

- prospective
- diagnostic or prognostic study
- performed at one institution


## References

- Bhatia KSS, King AD, Vlantis AC et al (2012) Nasopharyngeal mucosa and adenoids: appearance at MR imaging. *Radiology* 263:437–443
- Chan KCA, Woo JKS, King A et al (2017) Analysis of plasma Epstein-Barr virus DNA to screen for nasopharyngeal Cancer. *N Engl J Med* 377:513–522
- King AD, Vlantis AC, Bhatia KSS et al (2011) Primary nasopharyngeal carcinoma: diagnostic accuracy of MR imaging versus that of endoscopy and endoscopic biopsy. *Radiology* 258:531–537
- King AD, Wong LYS, Law BKH et al (2018) MR imaging criteria for the detection of nasopharyngeal carcinoma: discrimination of early-stage primary tumors from benign hyperplasia. *AJNR Am J Neuroradiol* 39:515–523
- Thoeny HC, De Keyzer F, King AD (2012) Diffusion-weighted MR imaging in the head and neck. *Radiology* 263:19–32
- Zhang SX, Jia QJ, Zhang ZP et al (2014) Intravoxel incoherent motion MRI: emerging applications for nasopharyngeal carcinoma at the primary site. *Eur Radiol* 24:1998–2004
- Le Bihan D, Breton E, Lallemand D et al (1988) Separation of diffusion and perfusion in intravoxel incoherent motion MR imaging. *Radiology* 168:497–505
- King AD, Lam WWM, Leung SF et al (1999) MRI of local disease in nasopharyngeal carcinoma: tumour extent vs tumour stage. *Br J Radiol* 72:734–741
- King AD, Bhatia KSS (2010) Magnetic resonance imaging staging of nasopharyngeal carcinoma in the head and neck. *World J Radiol* 2:159
- King AD, Vlantis AC, Yuen TWC et al (2015) Detection of nasopharyngeal carcinoma by MR imaging: diagnostic accuracy of MRI compared with endoscopy and endoscopic biopsy based on long-term follow-up. *AJNR Am J Neuroradiol* 36:2380–2385
- Yoshida T, Urikura A, Shirata K et al (2016) Image quality assessment of single-shot turbo spin echo diffusion-weighted imaging with parallel imaging technique: a phantom study. *Br J Radiol* 89:20160512
- Mikayama R, Yabuuchi H, Sonoda S et al (2018) Comparison of intravoxel incoherent motion diffusion-weighted imaging between turbo spin-echo and echo-planar imaging of the head and neck. *Eur Radiol* 26:316–324
- Sakamoto J, Imaizumi A, Sasaki Y et al (2014) Comparison of accuracy of intravoxel incoherent motion and apparent diffusion coefficient techniques for predicting malignancy of head and neck tumors using half-Fourier single-shot turbo spin-echo diffusion-weighted imaging. *Magn Reson Imaging* 32:860–866
- Liang L, Luo X, Lian Z et al (2017) Lymph node metastasis in head and neck squamous carcinoma: efficacy of intravoxel incoherent motion magnetic resonance imaging for the differential diagnosis. *Eur J Radiol* 90:159–165
- Sumi M, Van Cauteren M, Sumi T et al (2012) Salivary gland tumors: use of Intravoxel incoherent motion MR imaging for assessment of diffusion and perfusion for the differentiation of benign from malignant tumors. *Radiology* 263:770–777
- Tan H, Chen J, Zhao Y et al (2018) Feasibility of intravoxel incoherent motion for differentiating benign and malignant thyroid nodules. *Acad Radiol*. <https://doi.org/10.1016/j.acra.2018.05.011>
- Shen J, Xu X, Su G, Hu H (2018) Intravoxel incoherent motion magnetic resonance imaging of the normal-appearing parotid glands in patients with differentiated thyroid cancer after radioiodine therapy. *Acta Radiol* 59:204–211
- Lai V, Li X, Ho V et al (2013) Intravoxel incoherent motion MR imaging: comparison of diffusion and perfusion characteristics between nasopharyngeal carcinoma and post-chemoradiation fibrosis. *Eur Radiol* 23:2793–2801
- Mao J, Shen J, Yang Q (2016) Intravoxel incoherent motion MRI in differentiation between recurrent carcinoma and postchemoradiation fibrosis of the skull base in patients with nasopharyngeal carcinoma. *J Magn Reson Imaging* 44:1556–1564
- Jia QJ, Zhang SX, Chen WB et al (2014) Initial experience of correlating parameters of intravoxel incoherent motion and dynamic contrast-enhanced magnetic resonance imaging at 3.0 T in nasopharyngeal carcinoma. *Eur Radiol* 24:3076–3087
- Lai V, Li X, Lee VHF et al (2014) Nasopharyngeal carcinoma: comparison of diffusion and perfusion characteristics between different tumour stages using intravoxel incoherent motion MR imaging. *Eur Radiol* 24:176–183
- Xiao Y, Pan J, Chen Y et al (2015) Intravoxel incoherent motion magnetic resonance imaging as an early predictor of treatment response to neoadjuvant chemotherapy in locoregionally advanced nasopharyngeal carcinoma. *Medicine (Baltimore)* 94:e973

23. Xiao-Ping Y, Jing H, Fei-Ping L et al (2016) Intravoxel incoherent motion MRI for predicting early response to induction chemotherapy and chemoradiotherapy in patients with nasopharyngeal carcinoma. *J Magn Reson Imaging* 43:1179–1190
24. Yu X, Hou J, Li F et al (2016) Quantitative dynamic contrast-enhanced and diffusion-weighted MRI for differentiation between nasopharyngeal carcinoma and lymphoma at the primary site. *Dentomaxillofac Radiol* 45:20150317
25. Surov A, Ryl I, Bartel-Friedrich S et al (2015) Diffusion weighted imaging of nasopharyngeal adenoid hypertrophy. *Acta Radiol* 56: 587–591
26. Noij DP, Martens RM, Marcus JT et al (2017) Intravoxel incoherent motion magnetic resonance imaging in head and neck cancer: a systematic review of the diagnostic and prognostic value. *Oral Oncol* 68:81–91

**Publisher's note** Springer Nature remains neutral with regard to jurisdictional claims in published maps and institutional affiliations.

## Affiliations

Qi-Yong Ai<sup>1</sup> · Ann D. King<sup>1</sup>  · Janet S. M. Chan<sup>1</sup> · Weitian Chen<sup>1</sup> · K. C. Allen Chan<sup>2</sup> · John K. S. Woo<sup>3</sup> · Benny C. Y. Zee<sup>4</sup> · Anthony T. C. Chan<sup>5</sup> · Darren M. C. Poon<sup>5</sup> · Brigitte B. Y. Ma<sup>5</sup> · Edwin P. Hui<sup>5</sup> · Anil T. Ahuja<sup>1</sup> · Alexander C. Vlantis<sup>3</sup> · Jing Yuan<sup>6</sup>

<sup>1</sup> Department of Imaging and Interventional Radiology, The Chinese University of Hong Kong, Prince of Wales Hospital, 30-32 Ngan Shing Street, Sha Tin, New Territories, Hong Kong SAR, China

<sup>2</sup> Department of Chemical Pathology, State Key Laboratory Translational Oncology, Li Ka Shing Institute of Health Sciences, The Chinese University of Hong Kong, Prince of Wales Hospital, Shatin, New Territories, Hong Kong SAR, China

<sup>3</sup> Department of Otorhinolaryngology, Head and Neck Surgery, The Chinese University of Hong Kong, Prince of Wales Hospital, Shatin, New Territories, Hong Kong SAR, China

<sup>4</sup> Jockey Club School of Public Health and Primary Care, The Chinese University of Hong Kong, Shatin, New Territories, Hong Kong SAR, China

<sup>5</sup> Department of Clinical Oncology, State Key Laboratory Translational Oncology, The Chinese University of Hong Kong, Prince of Wales Hospital, Shatin, New Territories, Hong Kong SAR, China

<sup>6</sup> Medical Physics and Research Department, Hong Kong Sanatorium & Hospital, Happy Valley, Hong Kong SAR, China